First-principles study of the structural properties of MgS-, MgSe-, ZnS-, and ZnSe-based superlattices

Sun-Ghil Lee and K. J. Chang
Department of Physics, Korea Advanced Institute of Science and Technology, 373-1 Kusung-dong, Yusung-ku, Taejon, Korea
(Received 3 March 1995)

We perform self-consistent *ab initio* pseudopotential calculations to study the structural properties of Mg- and Zn-based binary compounds and the stability of MgSe-ZnSe ordered superlattices. For more ionic MgS and MgSe, the rocksalt structure is found to be more favorable over both the zinc-blende and wurtzite phases, while the zinc-blende structure is most stable for ZnS and ZnSe. Because of the imperfect d-orbital screening, the Zn-based compounds have smaller lattice constants and larger bulk moduli. For both the bulk and epitaxial MgSe-ZnSe superlattices ordered in the CuAu-I, CuPt, and chalcopyrite structures, the lattice mismatch between binary constituents gives rise to high strain energy, resulting in lattice instability against phase segregation into their binary components at $T = 0$. Similar lattice instabilities are also found for epitaxial common-anion $Mg_xZn_{1-x}S$ superlattices ordered in the chalcopyrite or famatinite structure. However, we find that common-cation MgS_ySe_{1-y} and ZnS_ySe_{1-y} superlattices grown on (001) GaAs and ordered in the chalcopyrite or famatinite structure are thermodynamically stable and exhibit the charge transfer from less ionic bonds to more ionic bonds, similar to the common-anion superlattices. Since the electronegativity of the S atom is higher than that for the Se atom, the charge transfer to the S atom compensates for the strain energy and stabilizes epitaxial superlattices.

I. INTRODUCTION

II-VI semiconductors and their heterostructures have been of growing interests because of their wide band gap character and the potential applications for optoelectronic devices. With a development of growing techniques, it is possible to make ZnS-ZnSe strained-layer superlattices.[1] However, in Zn-based semiconductors, only one type of doping is easily made: n-type doping for ZnSe, whereas p-type doping in ZnTe. Recently, $ZnSe_yTe_{1-y}$ or $Mg_yZn_{1-y}Se$ alloys were suggested to be promising materials for this purpose, because both p and n types of doping are easily achieved.[2] In fact, Morinaga and his co-workers found that ZnSe-based alloys with a small portion of Mg and S are doped easily for both p and n types, and they demonstrated the lasing operation based on these semiconductors.[3] Faschinger and his co-workers also suggested possible applications of $Mg_xZn_{1-x}Se_yTe_{1-y}$ alloys for optical devices.[4] In this respect, it is worthwhile to study the multilayer systems made of MgZn chalcogenides.

Compared to Mg (belongs to column IIA in the Periodic Table) based semiconductors, column-IIB compounds, such as ZnSe and ZnTe, are very different in the electronic and bonding properties. This difference was attributed to the existence of a metal d band inside the main valence band in column-IIB compound semiconductors. The role of d states in II-VI semiconductors was well studied.[5] The imperfect d orbital screening in group-IIB compounds make their atomic sizes and lattice parameters smaller than those for group-IIA compounds. Thus, the valence s orbitals in group-IIB elements are relatively tightly bonded, and this bond property leads to the tetrahedrally bonded structures, such as zinc-blende and wurtzite, while the rocksalt structure is more favorable for group-IIA elements. The absence of d orbitals in group-IIA elements results in lowering the valence band maximum and widening the band gap, thus, the superlattices made of ZnMg-VI and Zn-VI compounds were suggested to be type-I superlattices.[3] However, there has been less study for the stability of multilayer systems based on IIA-VI and IIB-VI semiconductors.

In this paper, we examine the structural properties of MgS, MgSe, ZnS, and ZnSe, using a first-principles pseudopotential method. The lattice constants, bulk moduli, and cohesive energies are calculated for the rocksalt, zinc-blende, and wurtzite structures. Because of the higher ionicity, the Mg-based compounds favor the rocksalt phase over both the zinc-blende and wurtzite phases. In the Zn-based compounds, the zinc-blende structure is most stable, and the lattice constants and bulk moduli are generally smaller than those for the Mg-based materials. We study the structural stability of bulk and epitaxial MgSe-ZnSe superlattices ordered in the CuAu-I, CuPt, and chalcopyrite structures. Since the superlattices considered here have a large lattice mismatch, the bulk formation enthalpies are found to be very high because of the increase of the strain energy, while the formation enthalpies are much reduced for epitaxially grown samples. We also find lattice instabilities for ternary common-anion MgS-ZnS superlattices ordered in the chalcopyrite or famatinite structure, similar to the MgSe-ZnSe system. However, we find a distinctive trend of stability for epitaxial common-cation MgS-MgSe and ZnS-ZnSe superlattices ordered in the chalcopyrite or famatinite structure; the charge transfer energy overcomes the strain energy, resulting in the lattice stability

0163-1829/95/52(3)/1918(8)/$06.00

against phase segregation into binary constituents. The stability of superlattices is discussed based on the electronegativity of atom and the ionicity of bond.

In Sec. II, we briefly describe the method of our calculations. In Sec. III, the results for the structural properties of binary compounds are given and discussed. The stability of ordered bulk and strained MgSe-ZnSe superlattices is discussed and compared with other common-anion MgS-ZnS superlattices and common-cation MgS-ZnS and MgSe-ZnSe superlattices ordered in the chalcopyrite or famatinite structure. Finally, we summarize the results in Sec. IV.

II. METHOD

The calculations are based on the first-principles pseudopotential method[6] within the local-density functional approximation (LDA).[7] The Wigner interpolation formula is used for the exchange and correlation potential.[8] Norm-conserving nonlocal pseudopotentials are generated by the scheme of Troullier and Martins[9] and transformed into the separable form of Kleinman and Bylander.[10] For the Zn pseudopotential, it is known that the inclusion of the Zn $3d$ states in the core shell results in a poor description of the ground state properties for ZnSe and ZnS.[5] With partial core corrections, however, the bulk properties for Zn-based compounds are found to be well described, compared to those obtained for the Zn potential with the $3d$ electrons in the valence shell (Zn_{3d}). In the calculations for Zn-based superlattices, we employ the Zn potential with partial core corrections only (Zn_{pcore}). The wave functions are expanded in a plane-wave basis set with a kinetic energy cutoff of 20 Ry throughout this work. Testing a higher cutoff energy of 25 Ry, the error in the total energy difference between the zinc-blende and wurtzite structures is found to be less than 1 meV per atom. For the Zn_{3d} potential, a cutoff energy of 64 Ry is used to ensure numerical convergence. To perform the Brillouin zone summation of the charge density, a set of special **k** points is employed for each structure, which is equivalent to the 10 **k** points in the irreducible sector of the zinc-blende Brillouin zone:[11] 12, 15, and 6 **k** points for the CuAu-I-like, CuPt-like, and chalcopyritelike structures, respectively. This choice of equivalent sets of **k** points ensures consistency in the comparison of the total energies between the ordered superlattices and the pure binary compounds. The energy functional is fully minimized by the modified-Jacobi relaxation method, which was recently developed and employed successfully for a variety of systems.[12] We further minimize the total energy by varying the lattice volume for bulk superlattices and the axial ratio for coherent epitaxial forms. Then, we relax internal ionic positions by calculating the Hellmann-Feynman forces[13] until the optimal atomic configuration is obtained.

We study the structural properties of binary compounds, MgS, MgSe, ZnS, and ZnSe, in the rocksalt, zinc-blende, and wurtzite structures. For bulk and epitaxially grown MgSe-ZnSe superlattices, we examine three different ordered structures: CuAu-I (CA), CuPt (CP), and chalcopyrite (CH) structures with long range orderings along the [001], [111], and [201] directions, respectively. For other ternary materials, $Zn_xMg_{1-x}S$, MgS_ySe_{1-y}, and ZnS_ySe_{1-y}, the chalcopyritelike and famatinitelike structures are considered and their structural stability is compared with that for $Zn_xMg_{1-x}Se$ ordered superlattices.

III. RESULTS

A. Structural properties of binary compounds

In II-VI semiconductors, the existence of a metal d band in the main valence band strongly affects the structural and electronic properties of these materials.[5] If the d^{10}-electron shell fully compensates electrostatically for the ten added protons in group-IIB elements, the valence properties of group-IIB compounds will be very similar to those for group-IIA compounds. However, the photoemission spectra and the band structure calculations showed a sizable coupling between the p- and d-electron shells in IIB-VI semiconductors, indicating that the d^{10}-electron shell does not fully screen the protons associated with those electrons.[5] Because of the p-d coupling, the valence p band is repelled, and the band gap is much reduced. As a result of incomplete d-orbital screening effects, the valence s electrons in group-IIB elements feel more attractive potential than for IIA elements and are more tightly bound, resulting in the smaller lattice constants and cohesive energies. Since group-IIB elements have higher electronegativities, the covalency of bonds in IIB-VI semiconductors is stronger, while the ionic character is prominent for IIA-VI semiconductors.

In Fig. 1, the calculated total energies are plotted as a function of lattice volume for four binary compounds, ZnS, ZnSe, MgS, and MgSe, in the rocksalt, zinc blende, and wurtzite structures. At zero pressure, the rocksalt phase is found to be most stable for MgS and MgSe, while the Zn-based compounds favor the zinc-blende structure. The charge asymmetry coefficient g of a cation-anion bond was suggested to be a measure of the ionic character of binary compounds and used to explain their stable structures.[14] The preference of the rocksalt phase in the Mg-based compounds over the zinc-blende is consistent with the picture that materials with higher g values favor more ionic structures like rocksalt (see Tables I and II). Furthermore, the stability of the wurtzite structure against the zinc-blende phase is also in good agreement with the general trend that for materials with higher g values the wurtzite phase is more stable. However, the energy differences between the rocksalt and zinc-blende phases in the Mg-based compounds are smaller than those found for the Zn-based compounds, and these results are reconciled with the earlier suggestion that MgS and MgSe may have a metastable fourfold coordinated structure.[15] In ZnS and ZnSe, since the g values are relatively lower, the zinc-blende structure is more stable than both the wurtzite and rocksalt structures. However, since the zinc-blende and wurtzite structures have similar

TABLE I. The lattice constants (a_0), bulk moduli (B_0), first derivatives of the bulk modulus (B_0'), cation-anion bond lengths (d), cohesive energies (E_c), and LDA band gaps (E_g) are listed for ZnS, ZnSe, MgS, and MgSe in the zinc-blende structure and compared with available experimental data. The charge asymmetry coefficients g (defined in Ref. 14) are given and the values in parentheses represent the results obtained from the Zn potential, with the d electrons in the valence shell.

Structure	Parameter	ZnS	ZnSe	MgS	MgSe
Zinc-blende	a_0 (Å)	5.436 (5.417)	5.688 (5.681)	5.584	5.873
		5.411[a]	5.669[a]		
	d (Å)	2.354 (2.346)	2.463 (2.460)	2.418	2.543
	B_0 (kbar)	774 (818)	639 (662)	575	470
		769[b]	625[b]		
	B_0'	3.5 (3.6)	3.8 (3.7)	3.7	4.0
	E_c (eV/atom)	3.85	3.48	4.49	3.99
		3.17[c]	2.63[c]		
	E_g (eV)	2.37	1.79	3.42	2.81
		3.82[d]	2.87[d]		3.6[e]
	g	0.67	0.60	0.79	0.73

[a]Reference 21.
[b]Reference 22.
[c]Reference 5.
[d]Reference 23.
[e]Reference 2.

tetrahedral bonds up to the second neighbor, the energy differences between these two structures in the Zn-based compounds are extremely small, of the order of meV per molecule, while they are about ten times larger for the Mg-based materials. As pressure increases, the rocksalt structure appears as a high pressure phase in both ZnS and ZnSe. Since the Zn-VI compounds have the metal d bands inside the valence band, we test the Zn pseudopotential with the d electrons in the valence shell. We find that the Zn_{3d} potential gives the total energy curves very similar to those obtained from the Zn_{pcore} potential as shown in Fig. 1; however, the energies for rocksalt

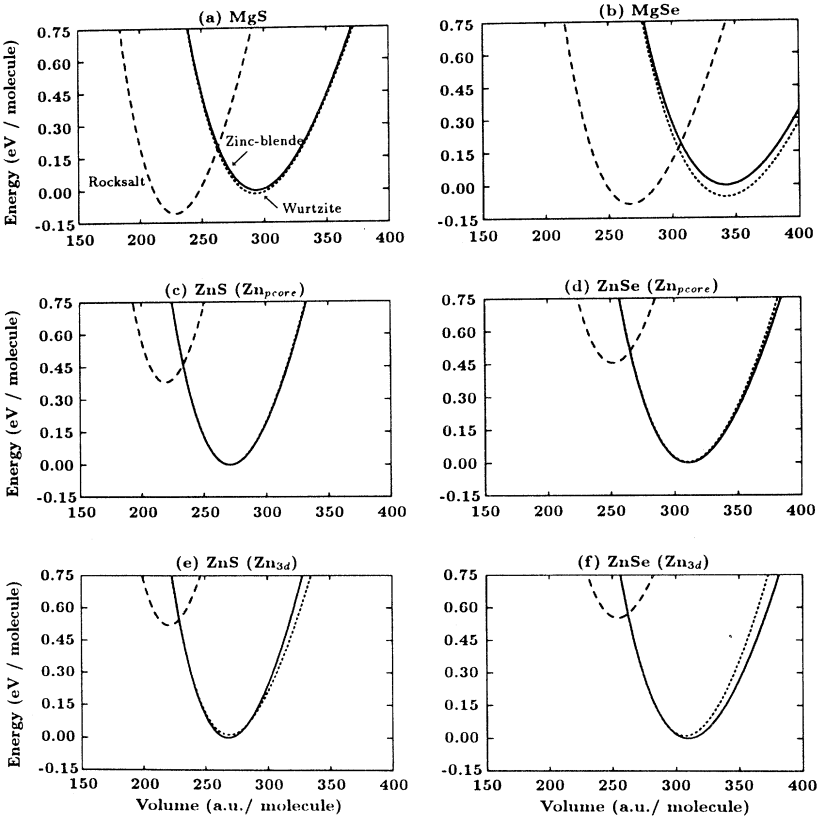

FIG. 1. Total energies (in units of eV per molecule) are plotted as a function of lattice volume for (a) MgS, (b) MgSe, (c) ZnS, and (d) ZnSe in the rocksalt (dashed), zinc-blende (solid), and wurtzite (dotted) structures. In (e) and (f), the Zn pseudopotential with the Zn 3d state in the valence shell is used.

TABLE II. The lattice constants (a_0 and c_0), bulk moduli (B_0), first derivatives of the bulk modulus (B_0'), and cation-anion bond lengths (d) are listed for ZnS, ZnSe, MgS, and MgSe in the rocksalt and wurtzite structures and compared with available experimental data. The equilibrium total energies (E_0) are calculated with respect to that for the zinc-blende phase. The values in parentheses represent the results obtained from the Zn potential with the d electrons in the valence shell.

Structure	Parameter	ZnS	ZnSe	MgS	MgSe
Rocksalt	a_0 (Å)	5.066 (5.079)	5.303 (5.320)	5.135	5.406
				5.203[a]	5.451[a]
	d (Å)	2.533 (2.539)	2.651 (2.660)	2.567	2.703
	B_0 (kbar)	1056 (1007)	864 (806)	777	627
	B_0'	3.7 (3.8)	3.9 (4.2)	3.5	4.2
	E_0 (meV/pair)	380 (520)	460 (550)	-110	-80
Wurtzite	a_0 (Å)	3.840 (3.828)	4.008 (3.989)	3.945	4.144
	c_0 (Å)	6.289 (6.279)	6.609 (6.598)	6.443	6.809
	d (Å)	2.354 (2.348)	2.463 (2.453)	2.416	2.543
	B_0 (kbar)	785 (719)	659 (739)	575	482
	B_0'	3.4 (4.5)	3.5 (3.3)	4.1	4.1
	E_0 (meV/pair)	1 (14)	5 (13)	-16	-52

[a]Reference 24.

ZnS and ZnSe with respect to the zinc-blende phase are generally increased by 0.14 and 0.09 eV per molecule, respectively. This results demonstrate that although the Zn_{pcore} potential provides the meaningful ground-state property for the zinc-blende structure, it does not describe properly the stability of high pressure phases, particularly, for the more ionic rocksalt phase.

The calculated lattice constants (a_0), bulk moduli (B_0), and first derivatives of the bulk modulus (B_0') are listed for the zinc-blende phase in Table I and for the rocksalt and wurtzite phases in Table II. The equilibrium lattice constants for ZnS and ZnSe are in good agreement with experimental values to within 0.5%, while the agreements (within 0.2 %) are better for the Zn_{3d} potential. As discussed earlier, although the Zn atom has one more electron shell than the Mg atom, the lattice constants for ZnS and ZnSe are smaller than those for the counterpart Mg-VI compounds, because of the more attractive potential resulting from the incomplete d-orbital screening effects. Furthermore, we find larger cohesive energies and band gaps for the Mg-VI compounds, which are attributed to the absence of the p-d coupling. For MgS and MgSe in the rocksalt phase, the calculated lattice constants are 5.135 and 5.406 Å, respectively, and these values agree with the measured values to within 1.3%. Although the rocksalt structure is only stable at high pressures for ZnS and ZnSe, their lattice constants are also found to be smaller than those for MgS and MgSe, similar to the zinc-blende structure.

B. MgSe-ZnSe superlattices

We first examine the structural properties of bulk MgSe-ZnSe superlattices ordered in the CuAu-I, CuPt, and chalcopyrite structures. The results for the lattice constants and the anion-cation bond lengths are listed and compared in Table III. Since the calculated lattice constants for zinc-blende ZnSe and MgSe are 5.688 and 5.873 Å, respectively, a lattice mismatch is estimated to be 3.27% between these two compounds. In the CuPt-like and chalcopyritelike structures, the lattice distortion along the ordering direction is found to be negligible, while in the CuAu-I-like structure the axial ratio is increased by 1.42% compared to its ideal value. We find that the equilibrium lattice constants satisfy the Vegard law to within 0.5% for all the ordered structures. Although the atomic positions are slightly distorted, the Zn-Se and MgSe bonds nearly recover their bulk bond lengths through internal atomic relaxations. In the CuAu-I-type superlattice, the Zn-Se and Mg-Se bond lengths are found to be larger by 0.4% and smaller by 0.2%, respectively, than those for the binary compounds. Similar deviations of the bond lengths are found for the Zn-Se (0.1% smaller) and Mg-Se (0.7% smaller) bonds in the chalcopyritelike structure. For the CuAu-I- and chalcopyritelike superlattices, each Se atom has an equal number of Zn-Se and Mg-Se bonds (see Fig. 2). However, in the CuPt-type superlattice, because of the asymmetric bonding configuration around each Se atom with respect to the (111) plane, there are two types of bonds, i.e., *on* and *off bonds*; the on bonds are aligned along the [111] direction, whereas the off bonds are off from the [111] orientation by the tetrahedral angle. In this structure, the bond lengths for the on bonds are somewhat close to those of the binary compounds to within 0.6%, while those for the off bonds deviate more. Similar results for the on and off bonds were also found for a InP-GaP superlattice in the CuPt-type structure.[18] When a superlattice is formed, a sizable amount of charge is transformed from the less ionic Zn-Se bond into the more ionic Mg-Se bond, as shown in Fig. 3. In both the

TABLE III. Cation-anion bond lengths (d) and bulk formation enthalpies (ΔH) are listed for three ordered MgSe-ZnSe superlattices. Three contributions to ΔH are given by the volume deformation (ΔE^v), charge transfer (ΔE^c), and relaxation energies (ΔE^r). In the CuAu-I structure, the lattice constants parallel to and perpendicular to the (001) plane are denoted by $a_0^{\parallel}$ and $a_0^{\perp}$, respectively. See the text for details of on and off bonds.

	CuAu-I	CuPt	Chalcopyrite
Ordering direction	[001]	[111]	[201]
a_0 (Å)	5.757 ($a_0^{\parallel}$)	5.758	5.756
	5.839 ($a_0^{\perp}$)		
$d_{\text{Mg-Se}}$ (Å)	2.538	2.540^{on}, 2.509^{off}	2.526
$d_{\text{Zn-Se}}$ (Å)	2.472	2.447^{on}, 2.478^{off}	2.460
ΔE^v (meV/atom)	11.3	10.2	10.2
ΔE^c (meV/atom)	4.3	3.5	4.0
ΔE^r (meV/atom)	-5.8	-3.8	-7.4
ΔH (meV/atom)	9.8	9.9	6.8

CuAu-I- and chalcopyrite-type structures, the increase of the charge density in a Mg-Se bond is almost equivalent to the decrease in a Zn-Se bond. In the case of the CuPt-type structure, however, an on bond has three times larger charge transfer than that for one of three off bonds. The reduction of the bond charge density causes a shorter bond length, because of the decrease of the screening effect and the more attractive interactions. Thus, the bond length of the Mg-Se on bond is larger than that for the off bond, while it is smaller for the Zn-Se on bond.

For a given structure, the stability of a bulk MgSe-ZnSe superlattice, with respect to phase segregation into binary constituents at $T = 0$, is tested by calculating the enthalpy of formation per anion-cation pair defined as

$$\Delta H(\text{Mg}_{0.5}\text{Zn}_{0.5}\text{Se}) = E^0(\text{Mg}_{0.5}\text{Zn}_{0.5}\text{Se}) - \frac{[E^0(\text{MgSe}) + E^0(\text{ZnSe})]}{2}, \quad (1)$$

where E^0 denotes the total energy in the equilibrium

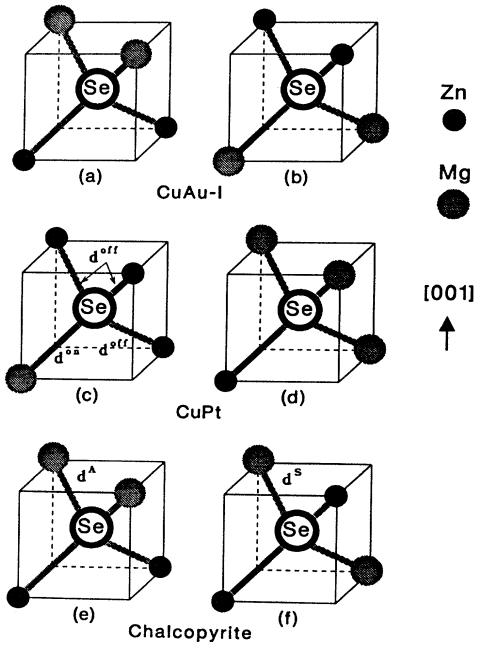

FIG. 2. Cation configurations around the Se atom in the MgSe-ZnSe superlattices ordered in the CuAu-I, CuPt, and chalcopyrite structures. See the text for details of d^{on}, d^{off}, d^A, and d^S.

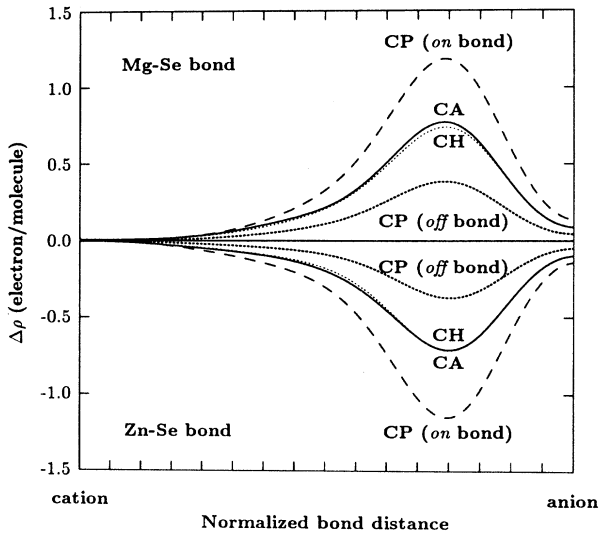

FIG. 3. For the MgSe-ZnSe superlattices, along the Mg-Se and Zn-Se bonds are plotted the differences between the valence charge densities in the CuAu-I, CuPt, and chalcopyrite structures and those for binary constituents in the zinc-blende structure. See the text for details of on and off bonds in the CuPt structure.

bulk structure. Here, we choose the zinc-blende structure as the equilibrium phase for MgSe. The results for the bulk formation enthalpies in the CuAu-I-, CuPt-, and chalcopyrite-type structures are listed in Table III. The formation enthalpy is found to be lowest for the chalcopyritelike structure, however, all the ordered structures considered here are unstable against phase segregation into binary constituents at $T = 0$. The stability of the ordered superlattices is found to be in the order of

$$\Delta H(\mathrm{CP}) > \Delta H(\mathrm{CA}) > \Delta H(\mathrm{CH}), \tag{2}$$

which is consistent with a general trend found in lattice-mismatched systems.[16] Testing the Zn_{3d} potential with the cutoff energies of 64 and 81 Ry, we find almost no change in the formation enthalpy for the CuAu-I-like and chalcopyritelike structures. However, in the CuPt-type phase, the formation enthalpy is lowered by about 2 meV per atom, thus, this structure becomes more stable than the CuAu-I-type structure.

To study more precisely the stability of superlattices, we examine three major contributions to ΔH:[17]

$$\Delta H = \Delta E^v + \Delta E^c + \Delta E^r, \tag{3}$$

where ΔE^v is the energy required to deform two constituents crystals into the equilibrium lattice constant of the superlattice, ΔE^c is the charge transfer energy caused by the ionicity difference between MgSe and ZnSe compounds when the superlattice is formed, and ΔE^r is the relaxation energy gained by releasing the atomic positions. As expected from the Vegard rule, the ordered structures considered here exhibit similar values for ΔE^v, with the maximum difference of about 1 meV per atom. However, ΔE^v is the largest contribution to the lattice instability, which is a general feature found in superlattices of lattice-mismatched constituents. The charge transfer energies are also found to be similar, however, our estimates for ΔE^c are larger by several times than those calculated in III-V pseudobinary compounds.[18,19] This large contribution from ΔE^c is attributed to the large ionicity difference between MgSe and ZnSe, which is caused by the presence of the $3d$ state in the Zn atom. The strains introduced by volume deformation are released by interatomic relaxations, resulting in the reduction of the formation enthalpy. In this process, since the cation-anion bond lengths are not fully recovered to their bulk constituent values, the superlattices are still thermodynamically unstable. The most release of strain is found for the chalcopyrite-type structure, thus, this structure has the lowest formation enthalpy. In the CuPt structure, because of the asymmetric bond geometry, the release of strain is smallest.

Next, we investigate the stability of epitaxially grown superlattices on three different (001) GaAs (a_0 = 5.654 Å), InP (a_0 = 5.869 Å), and InAs (a_0 = 6.036 Å) substrates. In this case, we consider thin pseudomorphic strained superlattices grown on a substrate, with the lattice constant $a_{\|}$ parallel to the substrate fixed to the substrate lattice constant and the lattice constant $a_{\perp}$ perpendicular to the substrate relaxed until an optimum geometry is obtained. Such grown superlattices experience uniaxial stress and lose the symmetry of the corresponding bulk superlattices if the ordering direction is not equivalent to the orientation of the substrate plane, particularly, for the CuPt- and chalcopyrite-type structures. Thus, for each Zn-Se and Mg-Se bond, there are two and three kinds of bond lengths for the epitaxial superlattices in the chalcopyrite and CuPt structures, respectively, as shown in Table IV. In the CuPt-type structure, the Zn-Se on bond oriented to the [111] direction is shortest in bond length, while the Mg-Se on bond is longest. For the off bonds, two types of bond lengths are found to be similar for each Zn-Se and Mg-Se bond.

TABLE IV. Cation-anion bond lengths (d) and epitaxial formation enthalpies (δH_{epi}) are listed for epitaxial MgSe-ZnSe superlattice ordered in the CuAu-I, CuPt, and chalcopyrite structures. Three different (001) GaAs, InP, and InAs substrates are considered. d and δH_{epi} are in units of Å and meV per atom, respectively. See the text and Fig. 2 for details of d^{on}, d^{off}, d^S, and d^A.

Structure		GaAs	InP	InAs
CuAu-I				
	$d_{\mathrm{Mg\text{-}Se}}$	2.529	2.528	2.558
	$d_{\mathrm{Zn\text{-}Se}}$	2.462	2.478	2.504
	δH_{epi}	6.1	7.4	6.7
CuPt				
	$d^{\mathrm{on}}_{\mathrm{Mg\text{-}Se}}$	2.535	2.543	2.569
	$d^{\mathrm{off}}_{\mathrm{Mg\text{-}Se}}$	2.506	2.520	2.542
		2.509	2.515	2.534
	$d^{\mathrm{on}}_{\mathrm{Zn\text{-}Se}}$	2.455	2.463	2.465
	$d^{\mathrm{off}}_{\mathrm{Zn\text{-}Se}}$	2.484	2.486	2.495
		2.481	2.492	2.505
	δH_{epi}	7.3	7.4	6.0
Chalcopyrite				
	$d^S_{\mathrm{Mg\text{-}Se}}$	2.531	2.540	2.572
	$d^A_{\mathrm{Mg\text{-}Se}}$	2.537	2.535	2.560
	$d^S_{\mathrm{Zn\text{-}Se}}$	2.463	2.467	2.485
	$d^A_{\mathrm{Zn\text{-}Se}}$	2.468	2.472	2.497
	δH_{epi}	4.1	4.7	3.3

In the chalcopyritelike structure, each cation-anion bond has two different bond lengths, because the Se atom has two different bonding geometries with the cations. In one configuration [see Fig. 2(e)] where the cation-anion bond length is denoted by d^A, the Mg and Zn atoms are separated by the (001) plane containing the Se atom, while in the other geometry [see Fig. 2(f)], the cations are mixed up on each side of the (001) plane with the bond length denoted by d^S. Independent of the type of superlattices, the bond length is found to increase as the lattice constant of a substrate increases.

In an epitaxially grown superlattice, the enthalpy of formation per cation-anion pair is defined similarly to the bulk form, except for the restriction that the in-plane lattice constant is fixed at its epitaxially confined value a_s:

$$\delta H_{\rm epi} = E_{\rm epi}(\mathrm{Mg_{0.5}Zn_{0.5}Se}, a_{\parallel} = a_s) - \frac{[E_{\rm epi}(\mathrm{MgSe}, a_{\parallel} = a_s) + E_{\rm epi}(\mathrm{ZnSe}, a_{\parallel} = a_s)]}{2}, \quad (4)$$

where $E_{\rm epi}(a_{\parallel} = a_s)$ denotes the equilibrium energy of a strained lattice. It is known that the epitaxial formation enthalpy $\delta H_{\rm epi}$ is generally smaller than the bulk value ΔH, because the binary constituents require additional volume deformation to form the strained lattice. The results for $\delta H_{\rm epi}$ are listed in Table IV. Although the formation enthalpies for the epitaxial superlattices are reduced by about 2–4 meV per atom compared with those for their bulk form, all the superlattices are still thermodynamically unstable against phase segregation into binary constituents at $T = 0$. For all the substrates considered here, the formation enthalpy is found to be lowest for the chalcopyrite-type structure. As the substrate changes to (001) InP, the formation enthalpy of the CuPt-type structure nearly equals that of the CuAu-I-type structure, while this structure is more stable than the CuAu-I-type phase on the InAs substrate.

C. $Zn_xMg_{1-x}S_ySe_{1-y}$ alloys

In this section, we discuss the stability of $Zn_xMg_{1-x}S_ySe_{1-y}$-based ordered superlattices. For simplicity, instead of studying quaternary alloys, we choose ternary superlattices epitaxially grown on a GaAs (001) surface: MgS_ySe_{1-y} ($x = 0$; $y = 1/4$, $1/2$, and $3/4$), ZnS_ySe_{1-y} ($x = 1$; $y = 1/4$, $1/2$, and $3/4$), $Zn_xMg_{1-x}Se$ ($x = 1/4$, $1/2$, and $3/4$; $y = 0$), and $Zn_xMg_{1-x}S$ ($x = 1/4$, $1/2$, and $3/4$; $y = 1$). Then, the lattice formation of the type of $A_{0.5}B_{0.5}C$ and $AB_{0.5}C_{0.5}$ is equivalent to the chalcopyrite-type structure, while the atomic configuration forms the famatinite-type structure for the type of $A_{0.25}B_{0.75}C$ and $AB_{0.25}C_{0.75}$. Despite the difference in composition ratio, the famatinite-type structure has the same [201] ordering as that of the chalcopyrite-type phase. Since our previous results showed that the chalcopyritelike structure is most stable among the ordered lattice-mismatched superlattices, we only consider the chalcopyrite- and famatinite-type structures for MgS_ySe_{1-y}, ZnS_ySe_{1-y}, $Zn_xMg_{1-x}Se$, and $Zn_xMg_{1-x}S$ alloys.

The calculated epitaxial formation enthalpies are given in Table V. We find a clear difference between the common-cation superlattices (CCS) and the common-anion superlattices (CAS); the epitaxially grown CCS's are thermodynamically stable against phase segregation into binary constituents at $T = 0$, while the CAS's are unstable. In lattice-mismatched bulk superlattices, it was shown that the elastic energy is generally greater by an order of magnitude than the charge transfer energy, resulting in the lattice instability. However, the elastic energy in epitaxially grown superlattices is significantly reduced, and it is comparable to the charge transfer energy as shown in Table V. Thus, the stability of epitaxial superlattices mainly depends on the charge transfer energy, because the elastic energy is normally positive. The negative charge transfer energies are found for the CCS's, while those for the CAS's are positive. Similar results were also found in other calculations for

TABLE V. Epitaxial formation enthalpies ($\delta H_{\rm epi}$) are compared for various $Zn_xMg_{1-x}S_ySe_{1-y}$-based ordered superlattices on (001) GaAs. Three contributions to $\delta H_{\rm epi}$ are given by the volume deformation ($\delta E^v_{\rm epi}$), charge transfer ($\delta E^c_{\rm epi}$), and relaxation energies ($\delta E^r_{\rm epi}$). Units are given in meV per atom.

(x, y)	$\delta E^v_{\rm epi} + \delta E^r_{\rm epi}$	$\delta E^c_{\rm epi}$	$\delta H_{\rm epi}$	
		Common-anion superlattices		
$(\frac{1}{4}, 1)$		0.0	1.9	1.9
$(\frac{2}{4}, 1)$		-0.8	2.2	1.4
$(\frac{3}{4}, 1)$		0.2	1.8	2.0
$(\frac{1}{4}, 0)$		0.7	3.0	3.7
$(\frac{2}{4}, 0)$		0.0	4.0	4.0
$(\frac{3}{4}, 0)$		2.0	3.1	5.1
		Common-cation superlattices		
$(1, \frac{1}{4})$		1.8	-2.3	-0.5
$(1, \frac{2}{4})$		3.4	-3.5	-0.1
$(1, \frac{3}{4})$		2.5	-2.7	-0.2
$(0, \frac{1}{4})$		-1.0	-1.0	-2.0
$(0, \frac{2}{4})$		0.3	-1.3	-1.0
$(0, \frac{3}{4})$		0.1	-1.2	-1.1

bulk superlattices.[18,19] When a superlattice is formed, the charge transfer between two different chemical bonds is governed by the ionicity difference; the charge flow occurs from the less ionic Zn-Se (or Zn-S) bond to the more ionic Mg-Se (or Mg-S) bond in the common-anion $Zn_xMg_{1-x}Se$ and $Zn_xMg_{1-x}S$ superlattices. The electronegativities for the Mg, Zn, Se, and S atoms were shown to be 1.18, 1.40, 1.96, and 2.12, respectively.[20] Since the electronegativity of Mg is smaller than that for Zn, the charge transfer from Zn to Mg increases the formation energy, resulting in positive charge transfer energies for the CAS's. In contrast, electron charges are transferred to the more electronegative S atom in the common-cation ZnS_ySe_{1-y} and MgS_ySe_{1-y} superlattices, because the charge flow occurs from the less ionic Zn-Se (or Mg-Se) bond to the more ionic Zn-S (or Mg-S) bond. Thus, the charge transfer energies for the CCS's are negative and exceed the elastic energies as seen in Table V.

Although our calculations are done for ordered ternary superlattices, our results indicate that it is possible to make stable $Zn_xMg_{1-x}S_ySe_{1-y}$ alloys lattice matched to the GaAs substrate, since the formation energy of a disordered alloy is close to that for the ordered chalcopyritelike structure. $Zn_xMg_{1-x}S_ySe_{1-y}$ and $Zn_xMg_{1-x}Se_yTe_{1-y}$ quaternary compounds were successfully grown and shown to be doped easily both n- and p-type compared to binary compounds.[2–4] Since a small portion of Mg increases the band gap, these alloys were suggested for suitable materials for optoelectronic devices.

IV. CONCLUSIONS

We have studied the structural properties of binary compounds, ZnS, ZnSe, MgS, and MgSe, and the stability of lattice-mismatched bulk and epitaxial ZnSe-MgSe superlattices using the first-principles pseudopotential method. We find that Mg-based compounds have higher ionicities and favor the rocksalt phase at zero pressure, while the zinc-blende phase is most stable for Zn-based materials. We have found that both the bulk and epitaxial ZnSe-MgSe superlattices in the CuAu-I, CuPt, and chalcopyrite structures are structurally unstable against phase segregation into binary constituents at $T = 0$. Although the charge flow from the less ionic Zn-Se bond to the more ionic Mg-Se bond is significant, this charge transfer increases the formation energy, because the electron charge is moved to the less electronegative Mg atom, which is caused by the absence of d orbital. Thus, the structural instability is mainly attributed to the excess elastic energy. The increase of the formation energy due to charge transfer is also found for the other common-anion $Zn_xMg_{1-x}S$ superlattices. However, for the common-cation MgS_ySe_{1-y} and ZnS_ySe_{1-y} superlattices, since the S atom has higher electronegativity than the Se atom, the charge transfer to the Mg-S or Zn-S bond gives rise to the decrease of the formation energy, stabilizing the ordered superlattices.

ACKNOWLEDGMENTS

This work was supported by the Ministry of Science and Technology and by the Korea Science and Engineering Foundation through the CMS at KAIST.

[1] T. Yokogawa, M. Ogura, and T. Kajiwara, Appl. Phys. Lett. **49**, 1702 (1986).
[2] D. J. Chadi, Phys. Rev. Lett. **72**, 534 (1994).
[3] Y. Morinaga, H. Okuyama, and K. Akimoto, Jpn. J. Appl. Phys. **32**, 678 (1993).
[4] W. Faschinger, S. Ferreira, and H. Sitter, Appl. Phys. Lett. **64**, 2682 (1994).
[5] S.-H. Wei and A. Zunger, Phys. Rev. B **37**, 8958 (1988).
[6] J. Ihm, A. Zunger, and M. L. Cohen, J. Phys. C **12**, 4409 (1979).
[7] W. Kohn and L. J. Sham, Phys. Rev. **140**, A1133 (1965).
[8] E. Wigner, Trans. Faraday Soc. **34**, 678 (1938).
[9] N. Troullier and J. L. Martins, Phys. Rev. B **43**, 1993 (1991).
[10] L. Kleinman and D. M. Bylander, Phys. Rev. Lett. **48**, 1425 (1982).
[11] S. Froyen, Phys. Rev. B **39**, 3168 (1989).
[12] C. H. Park, I.-H. Lee, and K. J. Chang, Phys. Rev. B **47**, 15 996 (1993).
[13] H. Hellmann, *Einführung in die Quantenchemie* (Deuticke, Leipzig, 1937); R. P. Feynman, Phys. Rev. **56**, 340 (1939).
[14] A. García and M. L. Cohen, Phys. Rev. B **47**, 4215 (1993).
[15] J. C. Phillips, *Bonds and Bands in Semiconductors* (Academic, New York, 1973).
[16] L. G. Ferreira, S.-H. Wei, and A. Zunger, Phys. Rev. B **40**, 3197 (1989).
[17] G. P. Srivastava, J. L. Martins, and A. Zunger, Phys. Rev. B **31**, 2561 (1985).
[18] C. H. Park and K. J. Chang, Phys. Rev. B **45**, 11 775 (1991).
[19] P. Boguslawski and A. Baldereschi, Phys. Rev. B **39**, 8055 (1989).
[20] J. St. John and A. N. Bloch, Phys. Rev. Lett. **33**, 1095 (1974).
[21] N. Kh. Abrikosov, V. B. Bankina, L. V. Poretskaya, L. E. Shelimova, and E. V. Skudnova, *Semiconducting II-VI, IV-IV, and V-VI Compounds* (Plenum, New York, 1969), p. 2.
[22] I. Broser *et al.*, in *Physics of II-VI and I-VII Compounds, Semimagnetic Semiconductors,* edited by O. Madelung, M. Schulz, and H. Weiss, Landolt-Börnstein, New Series, Group III, Vol. 17, Pt. b (Springer, Berlin, 1982), and references therein.
[23] W. H. Strehlow and E. L. Cook, J. Phys. Chem. Ref. Data **2**, 163 (1973).
[24] R. W. G. Wyckoff, *Crystal Structures* (Wiley, New York, 1963).